J. Chem. Sci., Vol. 117, No. 2, March 2005, pp. 145–151.

Fluorescence-enhancement with different ionic inputs in a cryptand-based multi-receptor signalling system

BAMAPRASAD BAG and PARIMAL K BHARADWAJ*
Chemistry Department, Indian Institute of Technology, Kanpur 208 016, India
e-mail: pkb@iitk.ac.in

Abstract. Two molecules of a laterally non-symmetric aza cryptand have been attached to 9,10-dimethylanthracene to obtain a multi-receptor fluorescent signalling system in the "receptor–spacer–fluorophore–spacer–receptor" format. In the absence of a metal ion, weak fluorescence is observed upon excitation of the anthryl group owing to efficient photo-induced electron transfer (PET) of the lone pair of N attached to the anthryl group. However, when a metal salt is added, the lone pair is engaged, thus in blocking of the PET and leading to recovery of fluorescence to different extents depending upon the nature of the metal ion.

Keywords. Fluorescence enhancement; photoinduced electron transfer; cryptand receptor; metal cryptate.

1. Introduction

Fluorescent signalling systems consist of signalling (fluorophore) and guest-binding (receptor) moieties. The two components can either be separated by a spacer or can be integrated into one unit with photo-induced intramolecular electron transfer (PET) being the commonly exploited mechanism.[1,2] Several reports are available on chelation-enhanced fluorescence[3–10] to make chemosensors for different types of metal ions. In this technique, the optical transduction of binding of metal ions with receptors is dependent upon the nature of the metal ion and its concentration, as well as the nature of the receptor. The fluorophore and the receptor are chosen such that the PET between the two (usually a group containing one or more nitrogen atoms) can be modulated. When the lone-pair associated with the donor atom is not bonded to a guest (in this case a metal ion or proton), PET from the receptor (i.e., N lone-pair) to the excited fluorophore takes place causing a non-radiative decay of the excited state and fluorescence-quenching. When a guest engages this lone-pair by bonding, the PET is blocked, causing recovery of the fluorescence. Both fluorescence-quenching and -enhancement can be utilized to obtain information about binding of the guest. However, the ubiquitous nature of fluorescence-quenching reduces its sensitivity, as well as its practical utility.[11,12] Therefore, systems with fluorescence-enhancement rather than quenching are preferred for designing signalling systems.

Transition metals are ubiquitous in nature and their detection is of importance in biological, clinical and environmental problems, while detection of heavy main-group metals and lanthanides is important from the perspectives of environmental pollution[13–15] and delayed luminescence[16–18] respectively. However, many of these metal ions, specially the paramagnetic transition metal ions, quench fluorescence very effectively through several pathways.[19,20] Blocking of the quenching pathways requires that metal–receptor (M–R) interactions should be considerably greater than the metal–fluorophore (M–F) communication.[21] Fluorescent signalling systems built in the format, 'fluorophore–spacer–receptor' with a cryptand as receptor is thus ideal because, once a metal ion enters the cavity of this receptor, it is isolated from the surroundings thus enabling it to nullify most, if not all, of the quenching pathways.[22] In the present studies, two cryptands are attached to anthracene via methylene spacers to get the multi-component fluorescent signalling system $\mathbf{L_1}$ (scheme 1) in the "receptor–spacer–fluorophore–spacer–receptor" format. This system is quite versatile, giving fluorescence-enhancement in the presence of a number of first-row transition metals, a number of lanthanides and several heavy main-group metals. Chemoselectivity of the cryptand to is too poor afford an *OR* logic gate. The present system can also offer a starting point for attachment of groups of interest through other derivatizable sites present in the cryptand.

Dedicated to the memory of the late Professor Bhaskar G Maiya
*For correspondence

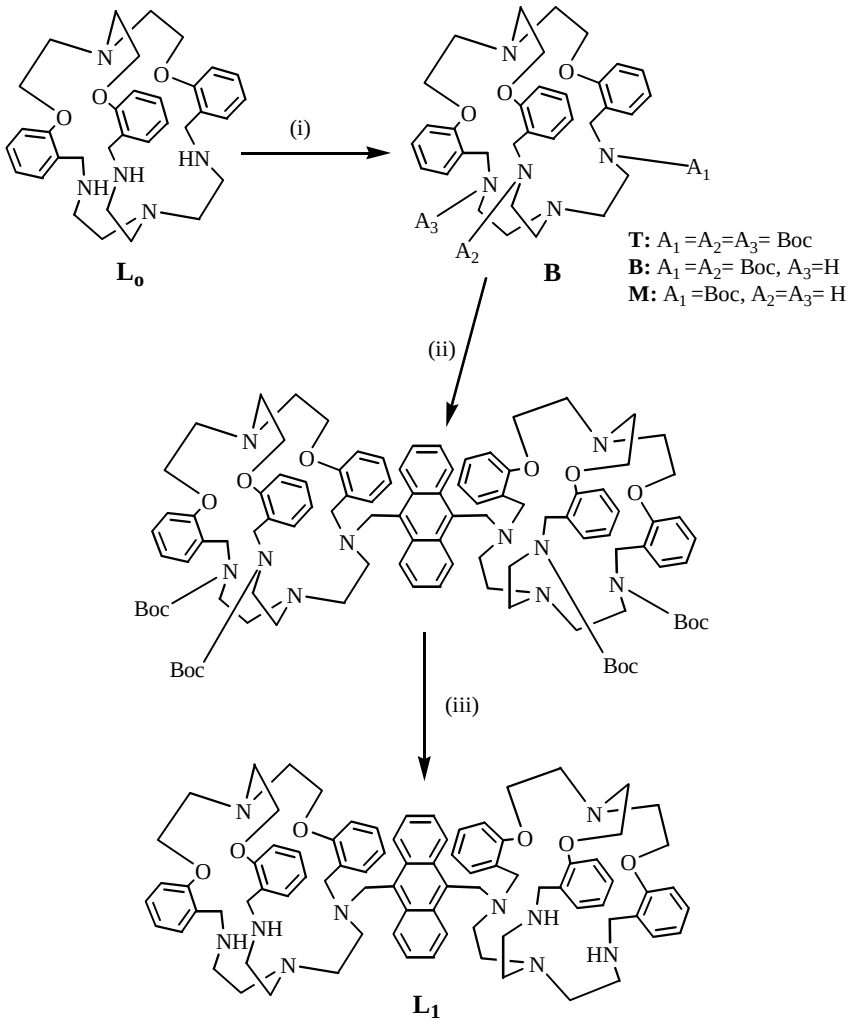

L_o **B** **L_1**

Reaction conditions: (i) Di-*t*-butyl di-carbonate, DCM, RT, 12 h. (ii) 9,10-*Bis*-(chloromethyl)anthracene, Et_3N, toluene, reflux, 50 h. (iii) Trifluoroacetic acid, 72 h, RT.

Scheme 1. Synthetic route to **L_1**.

2. Experimental

2.1 *Materials*

Cryptand **L_o**[23] was synthesized as reported earlier. All the solvents were freshly distilled prior to use and all the reactions were carried out under N_2 atmosphere unless otherwise mentioned. Chromatographic separation was done by column chromatography using 100–200 mesh silica gel obtained from Acme Synthetic Chemicals.

2.2 *Analysis and measurements*

The compounds were characterized by elemental analysis, ^{1}H-NMR, ^{13}C-NMR and mass (positive ion) spectroscopic studies. ^{1}H-NMR and ^{13}C-NMR spectra were recorded on a Jeol JNM-LA400 FT (400 MHz and 100 MHz respectively) instrument in $CDCl_3$ with Me_4Si as the internal standard. The electrospray mass spectra (ESI) were recorded in a Micromass Quatro II triple quadrupole mass spectrometer. Melting points were determined with an electrical melting point apparatus by Perfit, India and were uncorrected. Elemental analyses were obtained on an Elementar Vario EL III Carlo Erba 1108 elemental analyser. UV–visible spectra were recorded on a Jasco V-570 spectrophotometer in dry THF at 298 K. Fluorescence spectra were obtained with a Perkin–Elmer LS 50B luminescence spectrometer at 298 K. Solid-state emission was obtained with a Kimmon He–Cd Laser by exciting the solid samples at 325 nm.

Fluorescence quantum yield was determined in each case by comparing the corrected spectrum with that of anthracene in ethanol (f_F = 0·297) and taking the area under the total emission using the following equation,[24]

$$f_S = f_R\,(F_S A_R / F_R A_S).\,(h_S/h_R)^2, \qquad (1)$$

where f_S and f_R are the radiative quantum yields of the sample and the reference, F_S and F_R are the area under the fluorescence spectra of the sample and the reference, A_S and A_R are the absorbance of the sample and the reference (at the excited wavelength), h_S and h_R are the refractive indices of the solvents of the samples and the reference respectively.

2.3 *Synthesis*

Cryptand **L$_o$** was synthesized as reported earlier. Synthesis of the fluorophoric system was achieved in several steps as illustrated in scheme 1 and described as follows.

2.3a *Synthesis of bis-BOC protected cryptand*, **B**: The *bis*-protected cryptand was synthesized by partial derivatization of **L$_o$** with di-*t*-butyl dicarbonate. To a solution of **L$_o$** (1·68 g, 1 equiv., 3 mmol), in dichloromethane that was kept stirred, a solution of di-*t*-butyl dicarbonate (1·3 ml, 1·8 equiv., 5·4 mmol) in dichloromethane was added dropwise over a period of 30 min at 0°C after which it was allowed to stir for 12 h at RT. The solvent was removed under reduced pressure. The solid that remained was washed with water, extracted with $CHCl_3$, and after drying over anhydrous Na_2SO_4, was evaporated to dryness to obtain a mixture of *tris*-, *bis*- and *mono*-BOC protected **L$_o$** as a light brown solid. The components were separated through silica gel (100–200 mesh) column chromatography. The tri-substituted (**T**) cryptand was obtained in low yields (<10%) with 15–20% ethyl acetate in hexane as the eluent. The desired *bis*-protected cryptand (**B**) was obtained with 25% ethyl acetate in hexane as the eluent and upon evaporation afforded a brown crystalline solid.

Yield: 0·80 g (35%); m.p. 96°C; ^{1}H-NMR (400 MHz, $CDCl_3$, 25°C, TMS) *d*: (aliphatic) 1·4 (*s*, 18H), 2·2–2·8 (*m*, 13H), 3·2 (*br s*, 2H), 3·8 (*br s*, 6H), 3·9 (*br s*, 4H), 4·1 (*br s*, 2H), 4·4 (*br s*, 4H), (aromatic) 7·0 (*m*, 12H); ^{13}C-NMR (100 MHz, $CDCl_3$, 25°C, TMS) *d*: 28·4, 29·7, 45·2, 46·3, 48·7, 53·4, 54·6, 54·8, 67·4, 67·7, 68·4, 79·7 (aliphatic), 111·1, 111·5, 111·8, 120·9, 121·5, 126·9, 128·6, 130·2, 130·6, 131·0, 132·1, 154 (aromatic) 158·6 (C=O); ESI-MS *m*/*z* (%): 760 (100) [**B**]$^+$; Analysis – Calcd. for $C_{43}H_{61}N_5O_7$: C, 67·96; H, 8·09; N, 9·22%. Found: C, 67·87; H, 8·18; N 9·12%.

2.3b *Synthesis of* **L$_1$**: To a solution of **B** (0·76 g, 1 mmol) in dry toluene, triethylamine (0·6 ml, 4·3 mmol) was added and stirred for 30 min at RT. 9,10-*Bis*-(chloromethyl)anthracene[25] (0·14 g, 0·5 mmol) was added to this and the reaction mixture was heated to reflux for 50 h with constant stirring. It was then filtered and the filtrate distilled off under reduced pressure leaving behind a brown solid. The solid was washed with water, extracted with $CHCl_3$ and after drying over anhydrous Na_2SO_4, was completely evaporated under reduced pressure. The crude product thus formed was purified by passing through a column of neutral alumina with $CHCl_3$ and MeOH mixture (0·5 : 95·5 *v*/*v*) as the eluent to afford a brown solid. The solid was dissolved in minimum amount of THF and allowed to stir for 72 h at RT in excess tri-fluoroacetic acid (TFA). The solvent was then removed in a rotary evaporator to obtain a light brown semi-solid. After washing with a saturated solution of $NaHCO_3$ and NaCl, water (50 ml) was added to it and the desired product extracted with $CHCl_3$ (3 × 30 ml). Upon usual work-up followed by recrystallization from acetonitrile, **L$_1$** was obtained as a light brown solid.

Yield: 0·92 g (70%); m.p.: 128°C; ESI–MS, *m*/*z* (%): 1322 (55) [**L$_1$**]$^+$; Analysis – Calcd. for $C_{82}H_{100}N_{10}O_6$: C, 74·51; H, 7·63; N, 10·60%. Found: C, 74·42; H, 7·97; N 10·48%; ^{1}H NMR (400 MHz, $CDCl_3$, 25°C, TMS) *d*: (aliphatic) 2·1–2·6 (*m*, 28H [24H (CH_2), 4H (NH)]), 2·9–3·3 (*m*, 12H), 3·7 (*s*, 12H), 3·8 (*s*, 4H), 4·2–4·6 (*m*, 12H), (aromatic) 6·7–7·6 (*m*, 24H [Ph]), 7·9 (*m*, 4H, An-$H_{2,3,6,7}$), 8·3 (*d*, 2H, An-$H_{4,5}$), 8·7 (*d*, 2H, An-$H_{1,8}$); ^{13}C NMR (100 MHz, $CDCl_3$, 25°C, TMS) *d*: 154·2, 149·6, 135·4, 132·0, 130·5, 129·9, 127·1, 126·5, 125·8, 124·1, 123·4, 119·2, 115·8 (aromatic) 69·8, 63·6, 58·7, 56·2, 51·6, 48·9, 44·8, 42·1 (aliphatic).

3. Results and discussion

3.1 *UV–visible absorption spectroscopy*

In freshly purified THF, the parent cryptand and the metal cryptates show negligible absorption in the region of interest. The metal-free system exhibits the

characteristic peaks of 9,10-*bis*-alkyl substituted anthracene with (0,0) band at 397 nm and the vibrational structures at 378·0, 359·0, 340·0 nm. This indicates the absence of any interaction between the nitrogen lone pairs of the receptor and the anthracene group in the ground state. A similar observation was made[26] with the symmetrical trianthryl derivative of the cryptand. The X-ray crystallographic studies of the parent cryptands[27] and their Co(II), Ni(II), Cu(II), Zn(II), Ag(I), Pb(II) and Cd(II) cryptates reveal that these metal ions form mononuclear cryptates, occupying the lower deck of the cavity (i.e., tren-end) and the upper deck may sometimes be occupied by solvent molecules. For other transition metal ions, this binding mode can be inferred from spectroscopic data. X-ray data also show that the cryptands are mostly pre-organized and the conformational change is minimum when a metal ion enters the cavity. As a result, only a small red shift (Δl = 2–6 nm) in the peak position is observed when the ligand is complexed with a transition metal ion, whereas no shift in peak position is found with lanthanides as well as heavy metal ions such as Hg(II), Tl (I), Ag(I), except for Pb (II) where the shift in peak position is within 5 nm. The inner-transition metal ions, Eu(III) and Tb(III) prefer higher coordination[28] and may utilize all the donor atoms present in the cryptand. In such a case, these metal ions should occupy the middle of the cavity. Such a binding mode was found earlier with Cd(II).[29] All attempts to isolate lanthanide cryptates in single crystal form have remained unsuccessful.

3.2 *Emission spectra of cation-free L_1*

The cation-free system exhibits well-resolved anthracene $S_1 \rightarrow S_0$ emission in dry THF at 298 K with the (0,0) band at 408 nm along with vibrational structures at 458 and 430 nm. However, it does not exhibit any exciplex that appears as a structureless broad band around 550 nm in case of the trianthryl derivatives. This is because, in solution, interaction of the lone pair of donor N-atom with the *p* orbitals of the fluorophore is minimum in the present case. However, in the solid state, a broad band appears at ~550 nm that is assigned as the exciplex emission (figure 1). The quantum yield (f_F) of the monomer emission is found to be extremely low in the metal-free state attributable to a highly efficient PET process operative between the HOMO of the donor tertiary N atom and the anthracene *p* system. The quantum yield is found to be greater in a non-polar than in a polar solvent because the PET process is considerably enhanced[29,30] in a polar medium via charge–dipole and H-bonding interactions.

3.3 *Emission characteristics in presence of metal ions*

In presence of a metal ion, the emission spectrum shows a red-shift of the (0,0) band to within 5 nm, with broadening of both the (0,0) and other vibrational bands, and a different intensity ratio of the (0,0) and the first vibrational band as compared to that of the metal-free molecule. This slight red-shift is due to the metal ion-induced change in polarity around the fluorophore, whose emission band is solvatochromic in nature.

Upon complexation with a transition metal ion, emission intensity increases significantly. The extent of enhancement depends upon the nature of the metal ion. As the metal ion enters the cavity and binds the four N atoms at the tren-end, it effectively blocks the PET resulting recovery of fluorescence. Among the first-row transition metal ions studied, Zn(II) exhibits the highest enhancement due to its non-quenching nature and a favourable geometry for binding at the N_4-end of the cavity. On titration with Zn(II), the intensity of the emission band gradually increases and attains the maximum on addition of 2 equivalents of the metal ion (figure 2). The f_F vs stoichiometry plot with Zn(II) and Pb(II) indicates 2 : 1 complex formation. The fluorescence quantum

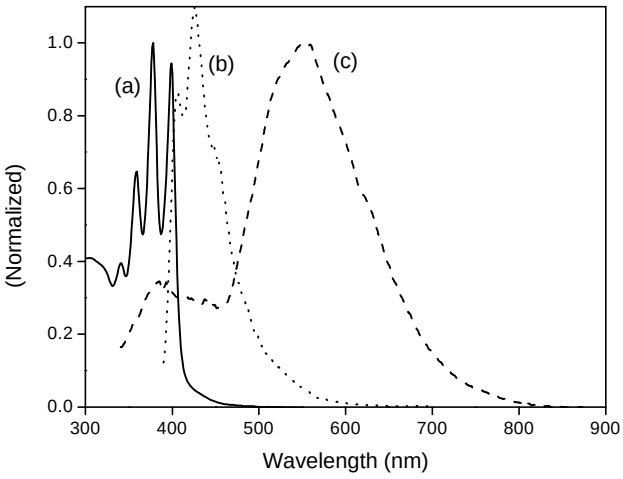

Figure 1. Normalized (a) absorption (——), (b) emission (·····) spectra of $\mathbf{L_1}$ in dry THF at 298 K and (c) emission spectra in solid state (-----).

Table 1. Band positions and molar extinction coefficients of the absorption transitions, fluorescence quantum yields and fluorescence-enhancement factors (FE) of the fluorophore $\mathbf{L_1}$ alone and in presence of various cationic inputs*.

Ionic input	l^{abs}_{max}, nm (e, $dm^3\ mol^{-1}\ cm^{-1}$)	Fluorescence output	
		f_F	*FE*
–	397(8107) 378(8582) 359(5527)	0·0023	1
Mn(II)	402(7624) 381(8531) 361(6322)	0·0772	34
Co(II)	399(5576) 378(5713) 358(5397)	0·0797	35
Ni(II)	401(8083) 380(8253) 361(5844)	0·0877	38
Cu(II)	402(4006) 381(4562) 362(4267)	0·1088	48
Zn(II)	402(7876) 380(8769) 361(8344)	0·2360	104
Pb(II)	402(8331) 381(8930) 362(7980)	0·1921	84
Ag(I)	399(7232) 378(7511) 358(6866)	0·0694	30
Hg(II)	399(6619) 378(7119) 359(4909)	0·0581	25
Tl(I)	400(7175) 379(7036) 361(4873)	0·0750	33
NH_4^+	399(7695) 377(8269) 358(5775)	0·0045	2
H^+	401(7560) 381(8425) 361(6186)	0·2596	118
Eu(III)	400(6208) 377(8170) 359(6339)	0·0818	36
Tb(III)	397(6828) 377(8170) 358(5798)	0·0524	23

**Experimental conditions*: Absorption spectra were taken in dry THF at 1×10^{-4} M concentration, RT. Fluorescence measurements: medium, dry THF; concentration of free ligand: 10^{-6} M; concentration of ionic input: 10^{-4} M; l_{ex} = 378 nm; excitation band-pass: 5 nm; emission band-pass: 5 nm; temperature: 298 K; f_{FT} calculated by comparison of corrected spectrum with that of anthracene (f_F = 0·297) taking the area under the total emission. Error in f_F is within 10% for the free ligand, otherwise 5% in each case.

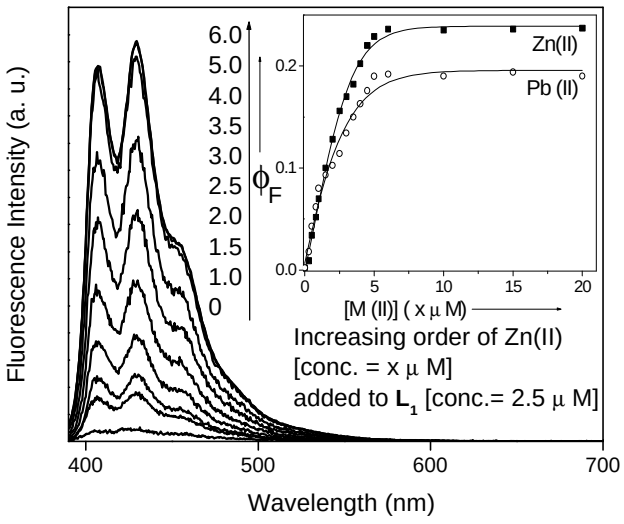

Figure 2. Fluorescence spectra of $\mathbf{L_1}$ as a function of added Zn(II) in dry THF at $2{\cdot}5 \times 10^{-6}$ M concentration. (Inset) Plot of fluorescence quantum yield (f_F) as a function of added metal concentration.

yields and extent of enhancements in presence of different metal ions are collected in table 1. The quenching abilities of transition and heavy metal ions are suppressed due to the entrapment of the metal ions inside the cryptand cavity leading to negligible M–F interactions.

We had earlier found[26,31] that the energy of the lowest triplet state of anthracene is lower than the emitting states of the Eu(III) and Tb(III) ions. Thus, there exists probable non-radiative decay of the excited singlet state of anthracene to its lowest triple state through the lanthanide(III) ion states. This energy transfer accounts for the observed lower f_F upon complexation with a lanthanide, compared to transition metal complexation. The present system exhibits substantial fluorescence recovery with heavy-metal ions. This is in contrast to the trianthryl cryptands where enhancement is observed only with Pb(II) ion. As the receptors in $\mathbf{L_1}$ are only partially derivatized, there is enough room for a heavy metal ion to enter the cavity, unlike in the case of the trianthryl cryptand, and cause recovery of fluorescence. For the heavy metal ions, the emission is structured with broadening of the bands. While both Ag(I) and Hg(II) show only slight enhancement, Pb(II) shows very high enhancement, probably due to a better fit of Pb(II) inside the cavity.

Protons generated from the hydrated metal perchlorate and nitrate salts in organic solvents can keep the lone pairs on the N atoms engaged through protona-

tion causing fluorescence enhancement. In order to verify that the fluorescence enhancement is caused by a metal ion and not by protonation, certain control experiments[7,26,32] are carried out. In the metal-free state, the f_{FT} either does not change or increases by a negligible amount on changing the solvent from dry THF to aqueous THF (THF: H_2O, 9 : 1 *v*/*v*) for all the systems. With a hydrated metal salt as input (1×10^{-3} M) in the medium THF: H_2O (9 : 1 *v*/*v*) the emission signal of $\mathbf{L_1}$ (1×10^{-5} M) enhances by a factor of 20–30 and does not change even after 48 h. This may be due to partial protonation of the N atoms attached to the anthryl group(s); the protons being generated by the metal salt in aqueous THF. However, in presence of $HClO_4$ (1×10^{-3} M), the fluorescence enhances by a factor of 118 in dry or aqueous THF medium. Besides, different metal ions provide different amounts of enhancement. If protons generated in the medium were responsible, then the enhancement factor should have been almost the same within experimental error for different metal ions.

4. Conclusion

The present study shows that fluorescent signalling with cryptand receptors is capable of exhibiting high fluorescence-enhancement in presence of metal ions of diverse nature. None of the fluorescence-quenching mechanisms are operational once a metal ion is in the cryptand cavity. In the case of trianthryl cryptands, metal ions such as Hg(II), Ag(I) and Tl(I) do not show any enhancement, apparently because these metal ions cannot enter the cavity of the *tris*-substituted receptor. Due to partial substitution, there is enough room for these ions to enter the cavity and effect strong enhancement. The high signal output in the present system is the result of a very effective PET process from the donor N to the fluorophore with concomitant low M–F interactions. The (0,0) band positions in the emission spectra do not change to any significant extent upon metal ion input. Hence, a potential *OR* logic gate can be built with this kind of molecules. Significantly, the cryptands still have one or two functionalizable sites which can be linked to molecules of interest to increase the scope(s) of this system. Cryptands make strong inclusion complexes with most of the metal ions, lowering their detection level if used as a sensor. If two different cryptands are attached to the anthryl moiety, different metal ions can selectively be incorporated in the cavities of these receptors leading to an *AND* logic gate. Our present efforts are directed along these lines.

Acknowledgement

Financial support for this work from the Department of Science and Technology, Govt. of India is gratefully acknowledged. BPB thanks the Council of Scientific and Industrial Research, New Delhi for fellowship.

References

1. Kavarnos G J 1993 *Fundamentals of photoinduced electron transfer* (Weinheim: VCH)
2. Czarnik A W 1997 *Chemosensors for ion and molecule recognition* (ed.) J-P Desvergne (Dordrecht: Kluwer)
3. de Silva A P, Gunaratne H Q N, Gunnlaugsson T, Huxley A J M, McCoy C P, Rademacher J T and Rice T E 1997 *Chem. Rev.* **97** 1515
4. Prodi L, Bolleta F, Montalti M and Zaccheroni N 2000 *Coord. Chem. Rev.* **205** 59
5. Rurack K and Resch-Genger U 2002 *Chem. Soc. Rev.* **31** 116
6. Szurdoki F, Ren D and Walt D R 2000 *Anal. Chem.* **72** 5250
7. Ramachandram B, Saroja G, Sankaran N B and Samanta A 2000 *J. Phys. Chem.* **B104** 11824
8. Valeur B and Leray I 2000 *Coord. Chem. Rev*. **205** 3
9. Fabbrizzi L and Poggi A 1995 *Chem. Soc. Rev*. **25** 197
10. Czarnik A W 1994 *Acc. Chem. Res*. **27** 302
11. Cammann K, Lemke U, Rohen A, Sander A, Wilken H and Winter B 1991 *Angew. Chem., Int. Ed. Engl*. **30** 516
12. Weiss S 1999 *Science* **283** 1676
13. Padilla-Tosta M E, Lloris J M, Martinez-Manez R, Marcos M D, Miranda M A, Pardo T, Sancenon F and Soto J 2001 *Eur. J. Inorg. Chem*. 1475
14. Xia W-S, Schmehl R H, Li C-J, Mague J T, Luo C-P and Guldi D M 2002 *J. Phys. Chem.* **B106** 833
15. Métivier R, Leray I and Valeur B 2003 *Chem. Commun*. 996
16. Parker D and Williams J A G 1998 *Chem. Commun*. 245
17. Gunnlaugsson T and Parker D 1998 *Chem. Commun*. 511
18. Gunnlaugsson T, Harte A J, Leonard J P and Nieuwenhuyzen M 2002 *Chem. Commun*. 2134
19. Kemlo J A and Shepard T M 1977 *Chem. Phys. Lett.* **47** 158
20. Varnes A W, Dodson R B and Wehry E L 1972 *J. Am. Chem. Soc*. **94** 946
21. Ramachandram B and Samanta A 1997 *Chem. Commun*. 1037
22. Bharadwaj P K 2003 *Prog. Inorg. Chem*. **51** 251

23. Ragunathan K G and Bharadwaj P K 1992 *Tetrahedron Lett.* **33** 7581
24. Uchiyama S, Matsumura Y, de Silva A P and Iwai K 2003 *Anal. Chem*. **75** 5926
25. Miller M W, Amidon R W and Tawney P O 1955 *J. Am. Chem. Soc*. **77** 2845
26. Ghosh P, Bharadwaj P K, Roy J and Ghosh S 1997 *J. Am. Chem. Soc*. **119** 11903
27. Sarkar B, Mukhopadhyay P and Bharadwaj P K 2003 *Coord. Chem. Rev*. **236** 1
28. Kepert D L 1987 In *Comprehensive coordination chemistry* (eds) G Wilkinson, R D Gillard and J A McCleverty (Oxford: Pergamon)
29. Bag B and Bharadwaj P K 2004 *Inorg. Chem*. **43** 4626
30. de Silva A P, Gunaratne H Q N, Habib-Jiwan J, McCoy C P, Rice T E and Soumillion J 1995 *Angew. Chem., Int. Ed. Engl*. **34** 1728
31. Das G, Bharadwaj P K, Basu Roy M and Ghosh S 2000 *J. Photochem. Photobiol.* **135** 7
32. Bag B and Bharadwaj P K 2004 *J Lumin*. **110** 85